Photoluminescence

Jaewon Jung[1]
[1] *Department of Physics and Astronomy, Seoul National University, Seoul 08858 Korea*
(Received 18 April 2024; revised 20 April 2024; accepted 24 April 2024; published 25 April)

Fluorescence, the important phenomenon of absorption and emission of photons by a material, provides numerous properties of the material such as impurities, phonon process, geometric configuration of the material, and band structure. We measure the photoluminescence signal from the Rhodamine 590 and the ruby crystal in different temperature, and pressure conditions and analyze the measured spectrum using the molecular band structure and the Debye theory. The experiment results closely align with the theoretical predictions such as the temperature dependence of the R-lines, Stokes sideband, and the transitions of vibrational states in Rhodamine 590.

I. INTRODUCTION

Luminescence, the process of converting energy into visible light, occurs when the substance is irradiated by various excitation sources. When the substance is excited by a light source, subsequently, photoexcitation happens and after diverse non-radiative relaxation processes, the sample emits the light. This phenomenon is known as photoluminescence (PL). The PL spectrum yields valuable information, such as the energy band structure, the geometric arrangement of the material, impurities or defects of the material, and its optical properties.

In this report, we measure the PL spectrum of Rhodamine 590, the molecule, and the ruby, the doped crystal, using monochromatic 532 nm laser source varying the temperature and pressure conditions. In addition, we analyze the properties of resulting emission spectra, mainly the peak heights, widths, and positions by using the Debye theory and Voigt integral.

A. Photoluminescence

Photoluminescence is a phenomenon wherein a material absorbs the incident photon, it emits light. It is classified into two branches, fluorescence and phosphorescence. In molecular systems, electrons exist in pairs since the unpaired ones are highly reactive and unstable. Therefore, the ground state is a singlet state and also the excited state is a singlet state due to the selection rule. When the electrons in the ground state absorb incident photons, they excite to the higher singlet state. They may or may not undergo non-radiative transition called intersystem crossing (ISC) before falling back to the ground state as illustrated in Fig. 1. If ISC occurs, the resulting emission process is known as fluorescence, typically characterized by a nanosecond lifetime. In contrast, if excited electrons fall back to the ground state without ISC, it is called phosphorescence with a much longer lifetime compared to fluorescence. Still, the excited electrons can undergo non-radiative internal conversion or vibrational relaxation.

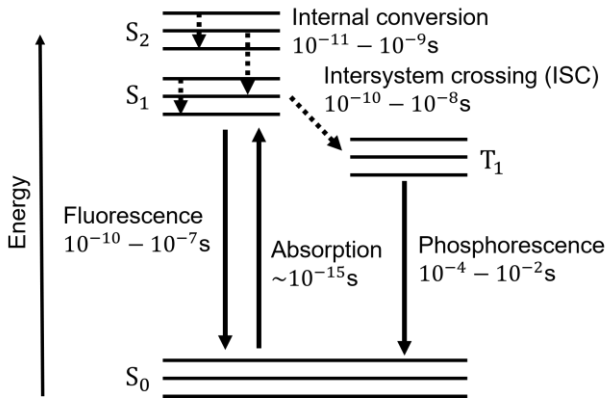

FIG. 1. Simple Jablonski diagram of photoluminescence. Time under the transition indicates the typical lifetime of each transition [1].

In experiment, the observed spectral lines are broadened that the peak in the spectrum is not a single valued. In other words, the peak has a linewidth which can be calculated from Voigt integral that involves a mixture of both homogeneous and inhomogeneous broadening. Voigt integral is defined as follows

$$V(x;\sigma,\gamma) = \int_{-\infty}^{\infty} G(x';\sigma)L(x-x';\gamma)dx', \quad (1)$$

where, $L(x;\gamma)$ ($G(x;\sigma)$) is a Lorentz (Gaussian) distribution, both distributions are normalized and centered to $x = 0$ and the x represents the shift from zero.

B. PL spectroscopy of Rhodamine 590

Rhodamine 590 or also known as Rhodamine 6G (R6G), is a fluorescent dye which is often used as a fluorescence tracer and a lasing medium. The PL emission spectrum ranges from 510 nm to 710 nm

with the peak typically around 550 nm which varies depending on the solvent and the dye concentration.

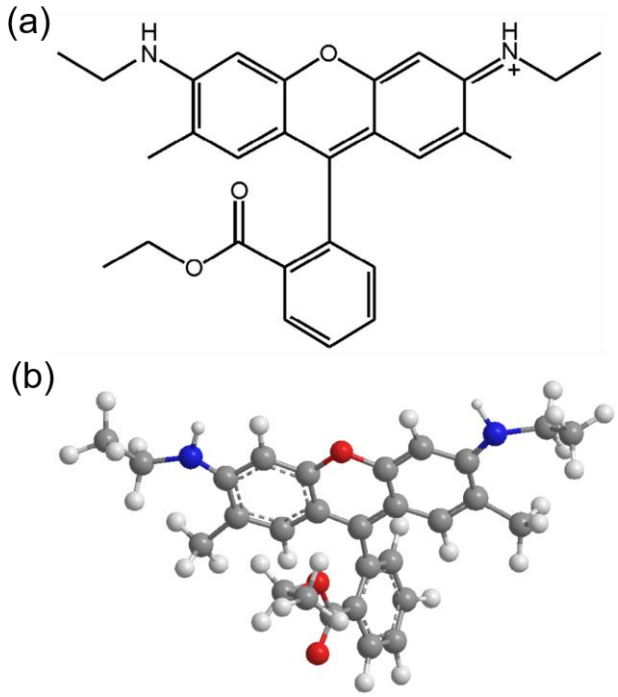

FIG. 2. (a) Chemical structure of Rhodamine 590 and (b) 3D geometry of Rhodamine 590 [2].

Fig. 2 shows that Rhodamine 590 has three benzene rings that form a fluorescence conjugated system. Using a linear combination of atomic orbitals (LCAO), the total Hamiltonian of Rhodamine 590 can be described by a linear combination of each orbital. However, exactly calculating the Hamiltonian of a molecule is computationally expensive and challenging. According to Kasha's rule, we can consider only the transition between the highest occupied molecular orbital (HOMO) and lowest unoccupied molecular orbital (LUMO) as shown in Fig. 3.

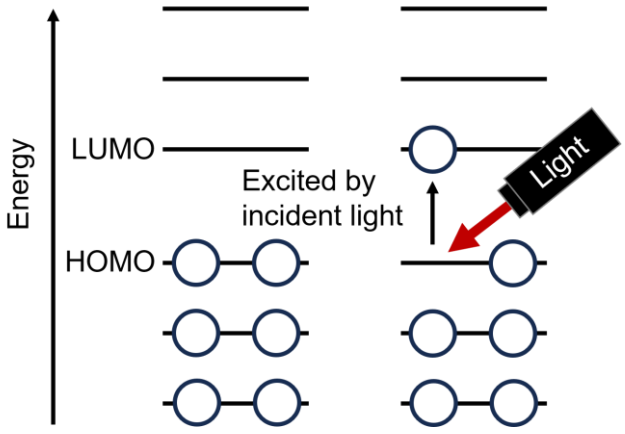

FIG. 3. Diagram of transition between LUMO and HOMO orbitals induced by incident light.

When the electrons excite to LUMO from HOMO, the fluorescence happens as the spontaneous emission occurs from LUMO to HOMO.

C. PL spectroscopy of Ruby

Ruby used in this experiment is a Cr^{3+} doped crystal, therefore, its PL spectrum cannot be explained in the same way as the molecule case in Rhodamine 590. Instead, the band theory holds for the crystal case. Based on the Debye theory, the ruby system can be analyzed using a four-level localized impurity system, and the corresponding phonon/impurity system can be represented by below Hamiltonian [3].

$$H = \sum_{n=0}^{3} \varepsilon_n \psi_n^\dagger \psi_n + \sum_k (\hbar v k)\left(a_k^\dagger a_k + \frac{1}{2}\right) + S_0\left\{C_{12}\psi_1^\dagger \psi_2 + \sum_{n=1,2} C_{n3}\psi_n^\dagger \psi_3 + c.c\right\} + S_0^2\left\{\sum_{n=0}^{2} d_n \psi_n^\dagger \psi_n + \left[d_{12}\psi_1^\dagger \psi_2 + c.c\right]\right\}, \quad (2)$$

where, ψ_n represents the impurity states and a_k represents the phonons. ε_n is eigenenergy of ψ_n such that $0 = \varepsilon_0 \ll \varepsilon_1 < \varepsilon_2 \ll \varepsilon_3$ and $(\varepsilon_1 - \varepsilon_0)$, $(\varepsilon_3 - \varepsilon_2) \gg \hbar\omega_d > \varepsilon_2 - \varepsilon_1$, ω_d is a Debye frequency, $d_n^* = d_n$, $S_0 = \sum_k (k/2v)^{\frac{1}{2}}(a_k + a_k^\dagger)$, and v is a sound velocity. There are two dominant lines in spectrum defined as R_1, R_2 lines which correspond to the transitions $1, 2 \leftrightarrow 0$ and positions are determined by Fourier transformation of the correlation function

$$F_n(\tau) = \langle[(\psi_n \psi_0^\dagger)(\tau), (\psi_0^\dagger \psi_n)]\rangle, \quad (3)$$

for n = 1, 2 and corresponding eigenenergy ε_n for n = 1, 2 are calculated by the perturbation theory as below

$$\varepsilon_n(T) = \varepsilon_n(0) + \alpha_n\left(\frac{T}{T_D}\right)^4 \int_0^{T_{D/T}} dx \frac{x^3}{e^x - 1} - \beta_{12}(-1)^n \frac{T_e}{T_D}\left(\frac{T}{T_D}\right)^2 \times \int_0^{\frac{T_D}{T}} dx \frac{x^3}{e^x - 1} \frac{P}{x^2 - \left(\frac{T_e}{T_D}\right)^2}, \quad (3)$$

and a width Γ_n is defined as

$$\Gamma_n(T) = \Gamma_n(0) + \bar{\alpha}_n\left(\frac{T}{T_D}\right)^7 \int_0^{\frac{T_D}{T}} dx \frac{x^6 e^x}{(e^x - 1)^2} \pi\beta_{12}\left(\frac{T_e}{T_D}\right)^3 \left[\delta_{n2} + \frac{1}{e^{T_e/T} - 1}\right], \quad (4)$$

where T_D is a Debye temperature, $T_e = \frac{\varepsilon_2 - \varepsilon_1}{k_B} = 42$ K for ruby and α_n, $\bar{\alpha}_n$, and β_{12} are as below

$$\alpha_n = \left[d_n - d_0 - \frac{|C_{n3}|^2}{\varepsilon_3 - \varepsilon_n} \right] \gamma_0,$$
$$\bar{\alpha}_n = \frac{2\pi}{\hbar\omega_D} [\alpha_n^2 + \left(|d_{12}|^2 + \frac{|C_{13}|^2 |C_{23}|^2}{(\varepsilon_3 - \varepsilon_1)(\varepsilon_3 - \varepsilon_2)} \right) \gamma_0^2,$$
$$\beta_{12} = \frac{|C_{12}|^2 \gamma_0}{\hbar\omega_D}, \quad (5)$$

where $\bar{\alpha}_n,\ \beta_{12} \geq 0$ and $\gamma_0 = 4\pi V(\omega_D)^4/[v^5(2\pi)^3]$. The β_{12} term represents direct-process of $R_1 \leftrightarrow R_2$ transition with the absorption or emission of a single phonon while the Raman terms, $\bar{\alpha}_n$ and α_n represents the scattering of the phonons due to the impurities.

The Cr^{3+} doped ruby is based on hexagonal closed-packed structure of Al_2O_3 with the impurity Cr^{3+} placed in it.

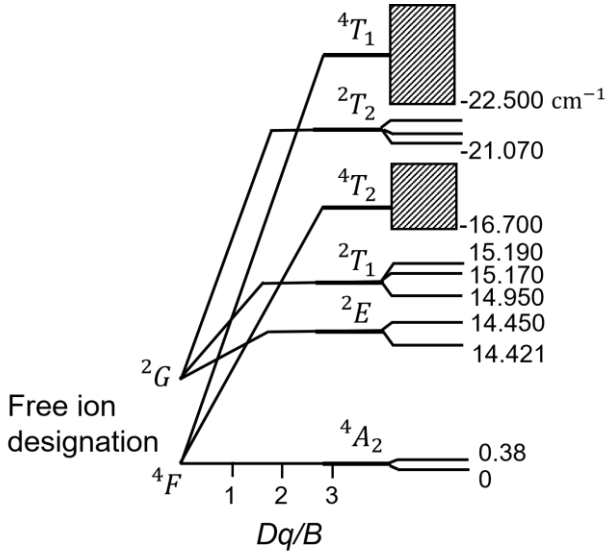

FIG. 4. Energy diagram [4] of Cr^{3+} ion in ruby versus the cubic field parameter Dq/B. $^4A_2$, ^2E, $^2T_1$, $^4T_2$ are the eigenstates of $\varepsilon_0, \varepsilon_1, \varepsilon_2, \varepsilon_3$, respectively. Dashed square box indicates energy bands.

From the energy diagram above, it can be concluded that the $\mathbf{Cr^{3+}}$ doped ruby crystal absorbs green light around 550 nm and the electrons excite from $^4\boldsymbol{A_2}$ to $^4\boldsymbol{T_2}$ and undergo non-radiative decay from $^4\boldsymbol{T_2}$ to $^2T_1$, $^2\boldsymbol{E}$ by phonons and emits R_1, R_2 lines from the transitions $^2T_1, ^2\boldsymbol{E} \rightarrow {}^4\boldsymbol{A_2}$.

II. METHODS

In this experiment, SLD-532-070T, the 532 nm laser, Dichroic filter, notch filter, cryostat, KDC2000F He compressor, LakeShore Model 335 Temperature Controller, DXG DM500i monochromator, Andor DU401A-BVF CCD, and Woosung Vacuum Co., Ltd. MVP24 rotary pump are used and the experimental setup is illustrated in Fig. 5. Measurements are done using the Andor Solis program and parameters used in the programs are tabulated in Table I.

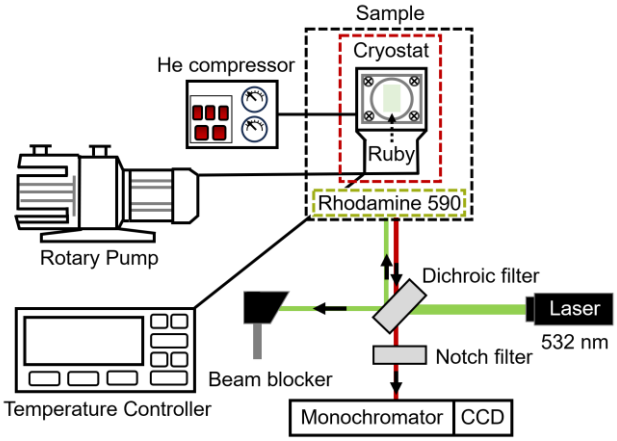

FIG. 5. Experimental setup for photoluminescence measurement. Black dashed box indicates the position of sample.

TABLE I. The parameters used in the experiment.

Parameters	Selected values
Center wavelength (nm)	567 (690): Rhodamine 590 (Ruby)
Accum cycle time (s)	0.01323
Exposure time (s)	0.1
Number of accumulations	15

The experiment procedure is outlined as follows. First, turn on all of the devices and set the parameters as in Table I. Then, PL spectrum measurements for (1) Rhodamine 590 at room temperature and atmospheric pressure, and (2) ruby from 8 K and 1 mTorr to room temperature and atmospheric pressure are conducted. For lowering the temperature and pressure in ruby experiment, the rotary pump is turned on at first. Once the pressure drops below 10 mTorr, the He compressor is turned on until the temperature reaches around 10 K. Around 200 K, the angle valve of the rotary pump is closed to prevent oil spillage. Then, utilize the heater to set the desired temperature and proceed with PL spectroscopy measurements.

Each measurement is acquired under thermal equilibrium conditions with a reduction of noise using the take background tool in the Andor Solis program and repeated 3 times for accuracy. The temperature of CCD is cooled down to around -30 ℃ to reduce thermal noise and the slit width is fixed around 0.20 mm which is calibrated in advance by TA.

III. RESULTS

Due to the malfunction of the cryo-system, the measurement results are not guaranteed to be executed under the desired temperature. Therefore, in this result section, we provide an estimated temperature for ruby results numerically obtained from the fluorescence results exploiting the fact that the intensity ratio of R1 and R2 lines are exponentially dependent on the temperature and the energy gap between them [6].

A. PL spectroscopy results of Rhodamine 590

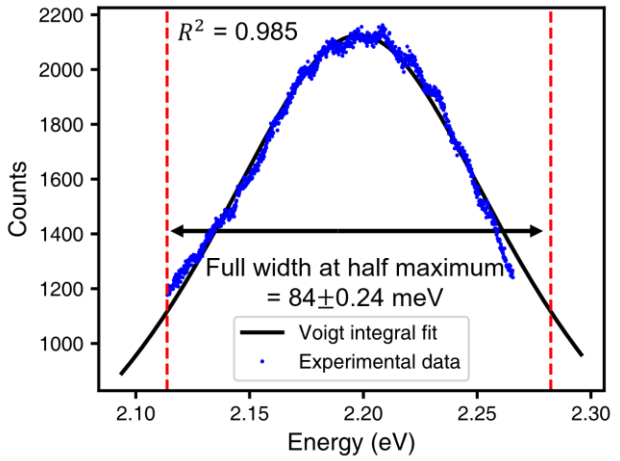

FIG. 6. Photoluminescence spectrum of Rhodamine 590 at the room temperature and atmospheric pressure fitted by Voigt integral. Red dashed lines represent the energy when the peak drops to half of its maximum.

The PL spectrum of Rhodamine 590 shows a Lorentzian peak at 2.208 eV with non-trivial wiggling patterns while the Gaussian contribution is smaller than the Lorentzian linewidth in the order of 10^6.

B. PL spectroscopy results of Ruby

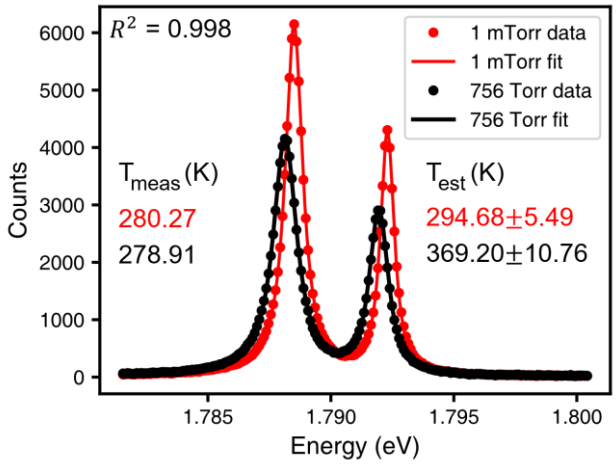

FIG. 7. R-line fluorescence spectra of Ruby crystal at 1mTorr and 756 Torr. T_{meas} (T_{est}) represents measured (estimated) sample temperature.

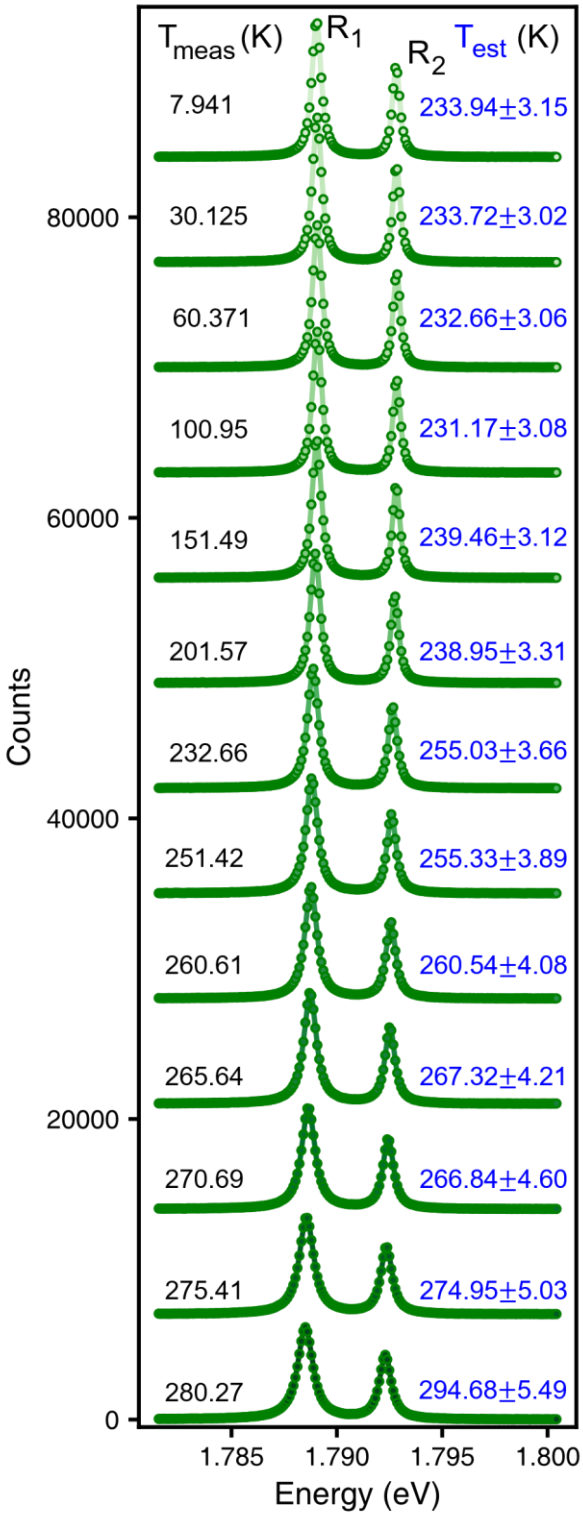

FIG. 8. R-line fluorescence spectra of Ruby crystal at 1 mTorr. T_{meas} (T_{est}) represents measured (estimated) sample temperature. The dots are the measurement results while the solid lines are fitted data using Voigt integral. Standard deviations of measured temperatures are less than 0.05 K. The R^2 values are 0.998 for all data. The error bars are smaller than the points. The emission lines are offset by 7000 counts.

The PL spectrum of ruby crystal is obtained at 13 different temperatures, and the measured data are fitted using bimodal Voigt integral. The estimated temperature is calculated using Eq. (6) [6]

$$\frac{I_2}{I_1} = \eta e^{-\frac{\Delta}{k_B T}}, \quad (6)$$

where $I_2(I_1)$ is the intensity of the $R_2(R_1)$ line, η is the quantum efficiency of the R_2 to the R_1 transition, and Δ is the energy gap between R_2 and R_1. The standard deviation of estimated temperature is obtained as [5]

$$\sigma = \sqrt{P + \frac{n}{2}B}, B = n\frac{N_1 + N_n}{2}, \quad (7)$$

where σ is a standard deviation of peak area P (intensity), n is the number of data points inside the peak area, and N_n is the counts for nth data point. The standard deviation of estimated temperature is then calculated using the error propagation technique.

From Fig. 7, it is observed that the R-lines tend to redshift and the peaks widen as the temperature increases. The high temperature of 369.20±10.76 K in Fig. 7 for 756 Torr is due to the increase of internal energy due to the high increase of pressure from 1 mTorr to 756 Torr. The pressure difference is not supposed to affect the R-lines unless the pressure is large as in the order of GPa that the peak difference in Fig. 7 is mostly due to the difference in temperature of the sample. Quantitative analysis regarding the temperature dependence of R-line shift, peak broadening, and the ratio of R-line peaks are discussed in the discussion section.

IV. DISCUSSIONS

A. PL spectrum of Rhodamine 590

The wiggling patterns

The Raman spectra of the Rhodamine 590 (R6G) in the Ethylen-glycol solvent range from 100 ~ 2000 cm^{-1} [7], therefore, the wiggling patterns in Fig. 6 are not expected to come from Raman scattering. Also, the dimer effects can [8] occur when the concentration of R6G changes which leads to the two different peaks of the R6G PL spectrum. However, since there are no double peaks nor overlap of the two peaks that the dimer effect didn't occur in our solvent. Still, the PL spectrum can be amplified or reduced according to the concentration, the greater the concentration, the greater the peak intensity and width. Thus, it is inferred that those patterns are due to the inhomogeneous concentration which can possibly induce irregular patterns on the resulting PL spectrum which can be further enhanced or varied by the solvent type and the dye concentration. Mostly, the local maxima in the patterns are due to the energy split of singlet states as discussed in next section which can result in slightly different peak intensity in the PL spectrum.

Estimation of the energy level

The energy level of Rhodamine 590 (R6G) can be further calculated from vibrational states of singlet states as shown in Fig. 9. The measured energy of the maximum peak is 2.208 eV which is consistent with the energy gap between S_1 and S_3 and the other local maxima are consistent with the earlier work in [9] as shown in Fig. 10. Therefore, the local maxima in wiggling patterns are verified that they came from the transition between vibrational states.

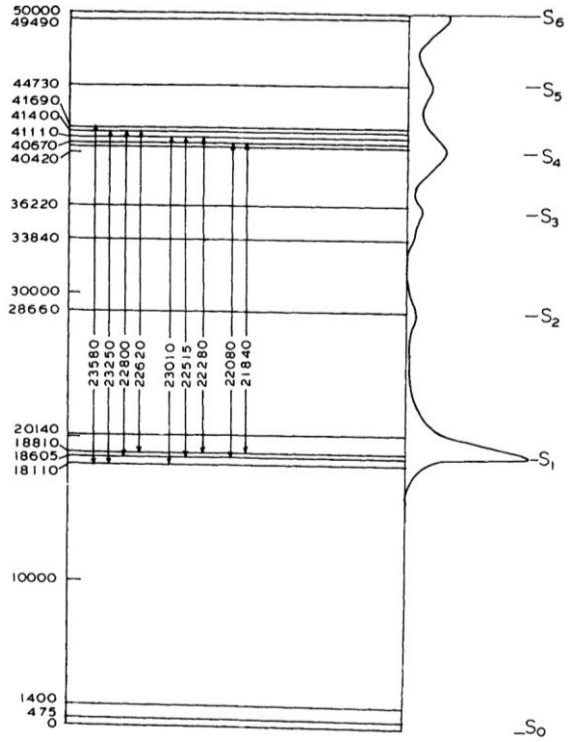

FIG. 9. Energy level diagram of singlet states in R6G in the units of **cm^{-1}** [9].

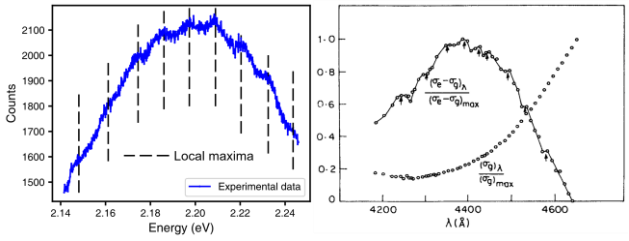

FIG. 10. Left: local maxima in R6G PL spectrum. Right: local maxima in normalized excited singlet state absorption spectrum of R6G [9].

B. PL spectrum of Ruby crystal

Temperature and pressure dependence

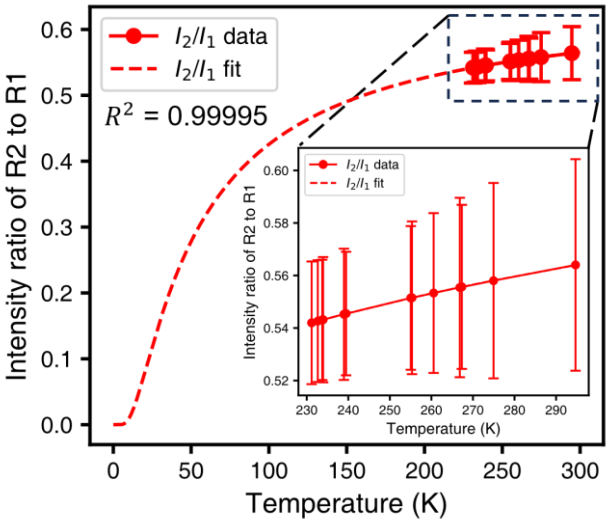

FIG. 11. Temperature dependence of intensity ratio of I_2 to I_1. The energy gap is obtained as $\boldsymbol{\Delta} = 3.66 \pm 5.72 \cdot 10^{-8}$ meV and the quantum efficiency $\eta = 0.6512 \pm 5.19 \cdot 10^{-8}$.

From the intensity ratio and using the Eq. (6), the temperature of sample is estimated as in Fig. 11. The measured energy gap and the quantum efficiency from the intensity ratio is also consistent with the theoretical values of 0.003582 eV at T = 300 K [3], $\boldsymbol{\eta}$ = 0.65±0.03 [6], and experimental values around 0.0037 eV in Fig. 12. Theoretically, since ruby has near degeneracy levels for R_1 and R_2 lines, it exhibits high Debye temperature around 700 ~ 900 K, accordingly, the quantum efficiency does not highly depend on the temperature below 100 K [6].

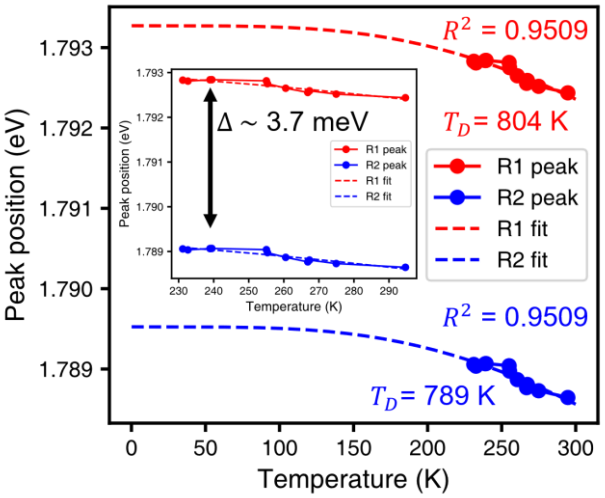

FIG. 12. Temperature dependence of R-lines peak positions. The measured energy gap is around 3.7 meV and the Debye temperature T_D is obtained as 804 (789) K for R_1 (R_2) peak. The error bars are smaller than the data points.

However, as the experiment condition was nearly room temperature that there is possibility of the quantum efficiency get affected. In addition, the doping rate of the ruby can also affect the Debye temperature and energy gap as well [11]. Here, as the measured Debye temperature, energy gap, and the quantum efficiency all shows agreement in theoretical values that this concern is not strictly considered in the analysis.

From Figs. 12-13, the Debye temperatures are calculated using Eqs. (3)-(5) and measured values range from 660 ~ 800 K which are in good agreement with experiment values in previous research [3-4, 6]. The fitted results of peak position in Fig.12 predict that the energy gap between R-lines doesn't change which is also consistent with the theory considering the Debye temperature ranges from 700 ~ 800 K. The redshift of the R-line peaks due to changes in temperature is well observed in Fig. 12. The fitted results of FWHM of R-lines well predict the zero width at T = 0 K while the other coefficients regarding the Raman terms or phonon scattering are poorly fitted since we lack low temperature data due to the cryo-stat issues.

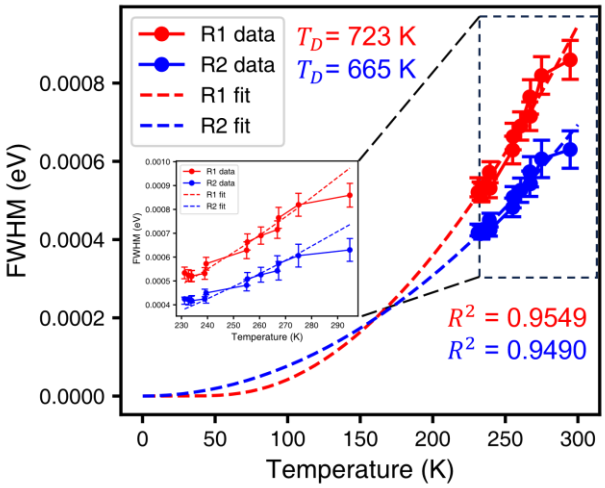

FIG. 13. Temperature dependence of full width at half maximum (FWHM) of R-lines. The Debye temperature T_D is obtained as 723(665) K for $R_1(R_2)$ peak.

Stokes sideband

The Stokes sideband or Stokes shift is the difference in energy between the absorption and emission spectra due to the occurrence of different transitions in vibrational states or dissipation in the solvent. When the electron absorbs the photon and transits to

the excited states, it emits the photon which has lower energy than the incident photon. The energy difference between incident and emitted photon induces Stokes shift and similar process occurs can happen in opposite which is called anti-Stokes shift.

Since the sample we use is solid ruby crystal that the stokes shift mostly comes from the vibrational relaxation and it is well observed in Fig. 14. There is also other contribution to the sideband other than the vibrational relaxation. In ruby, Cr^{3+} ions have exchange coupling and this coupling can induce sharp zero-phonon pair emission lines which are indicated with red triangles in Fig. 14.

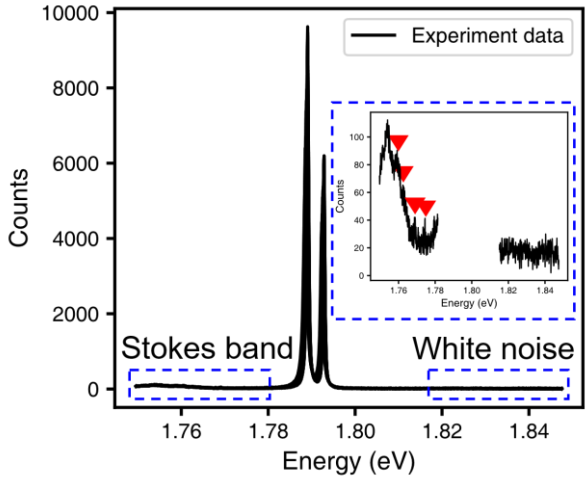

FIG. 14. The presence of Stokes side band in the ruby photoluminescence spectrum at room temperature and 1 mTorr. Red triangles indicate the peaks from zero-phonon emission induced from exchange coupling between $\mathbf{Cr^{3+}}$ ions.

C. Peak broadening

Peaks of the spectrum have linewidth due to various reasons. Based on the characteristic of broadening, the linewidth can be defined by Gaussian and Lorentzian shapes. The Gaussian part represents the inhomogeneous broadening due to the Maxwell-Boltzmann velocity distribution which leads to different velocities per each atom, therefore, Doppler broadening occurs differently for each atom that this type of broadening is inhomogeneous. On the other hand, the Lorentzian part represents the homogeneous broadening from diverse causes such as natural linewidth due to the spontaneous emission, power broadening, and collisional broadening.

In our experiment, R6G and ruby crystals show distinct linewidth shapes. In the R6G case, the linewidth is determined by various factors such as solvent effects, molecular dynamics, or temperature. In our room temperature experiment, its linewidth is mostly composed of the Lorentzian part since the Doppler broadening contribution is relatively small due to the low thermal velocities of atoms in solvent and high Lorentzian contribution from the changes in orientational intermolecular interactions due to the solvent [10]. In the ruby crystal case [3], the linewidth occurs due to the two main competing sources. First, in the low-temperature region, the inhomogeneous crystal strains play a dominant role which leads to homogeneous broadening. In contrast, the direct and Raman process results in inhomogeneous broadening as the temperature increases due to the increasing phonon densities. That is, both the homogeneous and inhomogeneous broadening competes and the ratio between them is dependent on the temperature region.

V. CONCLUSIONS

Here, we measure the photoluminescence (PL) line of the Rhodamine 590 (R6G) at room temperature and the Cr^{3+}-doped ruby crystal from low temperature to room temperature both in low pressure of 1mTorr and atmospheric pressure of 756 Torr. Using the cryo-stat along with the He compressor and rotary pump, the temperature and pressure are controlled for ruby spectroscopy measurement. However, the cryo-stat at the moment has a problem in lowering the temperature that the lowest measured temperature is estimated at around -40 ℃ and the low-temperature region is analyzed using the Debye theory-based energy and full width at half maximum (FWHM) equations in Eqs. (3)-(5).

The measured R6G PL spectrum shows a Lorentzian line shape in room temperature and the maximum peak position shows close energy with the theoretically predicted values. The local maxima from transitions between vibrational states are also precisely observed and verified with the previous experiment research.

The results for the ruby PL spectrum show good agreement with the theory that the peak location doesn't vary in low-temperature regions, the FWHM increases exponentially as the temperature increases, and the intensity ratio of R-lines give accurate energy gap and the quantum efficiency of the R_2 to the R_1 transition. Moreover, the Stokes sideband due to the vibrational relaxation as well as the small peaks from zero-phonon emission from exchange coupling between Cr^{3+} ions is well observed. Around 77 K, the FWHM of the R-lines show disagreement with the Debye theory due to the increasing contribution of inhomogeneous crystal strain, but due to the cryo-stat issues, it cannot be measured in this experiment. The

PL spectrum of both R6G and ruby can be further explored if we can measure the lifetime of the PL signal so that the origin of the luminescence can be verified.

ACKNOWLEDGEMENTS

The author would like to thank our teammates, Juwon Choi, Hyeonsung Jo, and Junyoung Lee for conducting this experiment together and having invaluable discussions during and after the experiment time. The author also would like to appreciate TA for supporting the initial start of the cryogenic instrument setting and the maintenance of all the devices used in the experiment.

REFERENCES

[1] Turro, Nicholas J., Vaidhyanathan Ramamurthy, and Juan C. Scaiano. *Principles of molecular photochemistry: an introduction*. University science books, 2009.
[2] Zehentbauer, Florian M., et al. "Fluorescence spectroscopy of Rhodamine 6G: Concentration and solvent effects." *Spectrochimica Acta Part A: Molecular and Biomolecular Spectroscopy* 121, 147-151 (2014).
[3] McCumber, D. E., and M. D. Sturge. "Linewidth and temperature shift of the R lines in ruby." *Journal of Applied Physics* 34.6, 1682-1684 (1963).
[4] Calviello, J. A., Fisher, E. W., & Heller, Z. H. (1966). Direct 2 T 1− 2 E Phonon Relaxation in Ruby and Its Effect Upon R-Line Breadth. *Journal of Applied Physics*, *37*(8), 3156-3160 (1966).
[5] Végh, János. "On calculating intensity from XPS spectra." *Journal of electron spectroscopy and related phenomena* 151.1, 24-30 (2006).
[6] Weinstein, B. A. "Ruby thermometer for cryobaric diamond-anvil cell." *Review of Scientific Instruments* 57.5, 910-913 (1986).
[7] Watanabe, Hiroyuki, et al. "DFT vibrational calculations of rhodamine 6G adsorbed on silver: analysis of tip-enhanced Raman spectroscopy." *The Journal of Physical Chemistry B* 109.11, 5012-5020 (2005).
[8] Sugiarto, I. T., and K. Y. Putri. "Analysis of dual peak emission from Rhodamine 6G organic dyes using photoluminescence." *Journal of Physics: Conference Series*. Vol. 817. No. 1. IOP Publishing, (2017).
[9] Venkateswarlu, Putcha, et al. "Transient excited singlet state absorption in Rhodamine 6G." *Pramana* 28, 59-71 (1987).
[10] Akimov, A. I., et al. "Lasing characteristics of solutions of rhodamine 6G and coumarin 47 with inhomogeneously broadened spectra." *Journal of Applied Spectroscopy* 37.2, 904-908 (1982).
[11] Cossolino, L. C., and Antonio Ricardo Zanatta. "Influence of chromium concentration on the optical–electronic properties of ruby microstructures." *Journal of Physics D: Applied Physics* 43.1, 015302 (2009).